Appendix

Table of Contents

List of Tables

List of Figures

A Environment & Task Details

A.1 MAZE

Description. A point-maze agent in a 2D maze learns to navigate from its start location to a goal location by iteratively predicting its x and y acceleration. The 6D states include the agent's two-dimensional current location and velocity, and the goal location. The start and the goal locations are randomized when an episode is initialized.

Evaluation. We evaluate the agents with 100 episodes and three random seeds and compare our method with the baselines regarding the average success rate and episode lengths, representing the effectiveness and efficiency of the policy learned by different methods. An episode terminates when the maximum episode length of 400 is reached.

Expert Dataset. The expert dataset consists of the 100 demonstrations with $18,525$ transitions provided by Lee et al. [2021].

A.2 FETCHPICK & FETCHPUSH

Description. FETCHPICK requires a 7-DoF robot arm to pick up an object from the table and move it to a target location; FETCHPUSH requires the robot arm to push an object to a target location. Following the environment setups of Lee et al. [2021], a 16D state representation consists of the angles of the robot joints, the robot arm poses relative to the object, and goal locations. The first three dimensions of the action indicate the desired relative position at the next time step. For FETCHPICK, the fourth dimension of action specifies the distance between the two fingers of the gripper.

Evaluation. We evaluate the agents with 100 episodes and three random seeds and compare our method with the baselines regarding the average success rate and episode lengths. An episode terminates when the agent completes the task or the maximum episode length is reached, which is set to 50 for FETCHPICK and 120 for FETCHPUSH.

Expert Dataset. The expert dataset of FETCHPICK consists of 303 trajectories ($10k$ transitions) while the expert dataset of FETCHPUSH consists of 185 trajectories ($10k$ transitions) provided by Lee et al. [2021].

A.3 HANDROTATE

Description. HANDROTATE Plappert et al. [2018] requires a 24-DoF Shadow Dexterous Hand to in-hand rotate a block to a target orientation. The 68D state representation consists of the joint angles and velocities of the hand, object poses, and the target rotation. The 20D action indicates the position control of the 20 joints, which can be controlled independently. HANDROTATE is extremely challenging due to its high dimensional state and action spaces. We adapt the experimental setup used in Plappert et al. [2018] and Lee et al. [2021], where the rotation is restricted to the z-axis and the possible initial and target z rotations are set within $[-\frac{\pi}{12}, \frac{\pi}{12}]$ and $[\frac{\pi}{3}, \frac{2\pi}{3}]$, respectively.

Evaluation. We evaluate the agents with 100 episodes and three random seeds and compare our method with the baselines regarding the average success rate and episode lengths. An episode terminates when the agent completes the goal or the maximum episode length of 50 is reached.

Expert Dataset. To collect expert demonstrations, we train a SAC Haarnoja et al. [2018] policy using dense rewards for $10M$ environment steps. The dense reward given at each time step t is $R(s_t, a_t) = d_t - d_{t+1}$, where d_t and d_{t+1} represent the angles (in radian) between current and the desired block orientations before and after taking the actions. Following the training stage, the SAC expert policy achieves a success rate of 59.48%. Subsequently, we collect 515 successful trajectories ($10k$ transitions) from this policy to form our expert dataset for HANDROTATE.

A.4 WALKER

Description. WALKER requires an agent to walk toward x-coordinate as fast as possible while maintaining its balance. The 17D state consists of angles of joints, angular velocities of joints, and velocities of the x and z-coordinate of the top. The 6D action specifies the torques to be applied on each joint of the walker avatar.

Evaluation. We evaluate each learned policy with 30 episodes and three random seeds and compare our method with the baselines regarding the average returns of episodes and episode lengths. The return of an episode is accumulated from all the time steps of an episode. An episode terminates when the agent is unhealthy (*i.e.*, ill conditions predefined in the environment) or the maximum episode length (1000) is reached.

Expert Dataset. The expert dataset consists of 5 trajectories with $5k$ state-action pairs provided by Kostrikov [2018].

B Algorithm

Our proposed framework DBC is detailed in Algorithm 1. The algorithm consists of two parts. (1) **Learning a diffusion model**: The diffusion model ϕ learns to model the distribution of concatenated state-action pairs sampled from the demonstration dataset D. It learns to reverse the diffusion process (*i.e.*, denoise) by optimizing $\mathcal{L}_{\text{diff}}$. (2) **Learning a policy with the learned diffusion model**: We propose a diffusion model objective $\mathcal{L}_{\text{DM}}$ for policy learning and jointly optimize it with the BC objective $\mathcal{L}_{\text{BC}}$. Specifically, $\mathcal{L}_{\text{DM}}$ is computed based on processing a sampled state-action pair (s, a) and a state-action pair $(s, \hat{a})$ with the action $\hat{a}$ predicted by the policy π with $\mathcal{L}_{\text{diff}}$.

Algorithm 1 Diffusion Model-Augmented Behavioral Cloning (DBC)

Input: Expert's Demonstration Dataset D
Output: Policy π.

// Learning a diffusion model ϕ
Randomly initialize a diffusion model ϕ
for each diffusion model iteration **do**
  Sample (s, a) from D
  Sample noise level n from $\{0, ..., N\}$
  Update ϕ using L_{diff} from Eq. 2
end for
// Learning a policy π with the learned diffusion model ϕ
Randomly initialize a policy π
for each policy iteration **do**
  Sample (s, a) from D
  Predict an action $\hat{a}$ using π from s: $\hat{a} \sim \pi(s)$
  Compute the BC loss L_{BC} using Eq. 1
  Sample noise level n from $\{0, ..., N\}$
  Compute the agent diffusion loss $L_{\text{diff}}^{\text{agent}}$ with $(s, \hat{a})$ using Eq. 3
  Compute the expert diffusion loss $L_{\text{diff}}^{\text{expert}}$ with (s, a) using Eq. 4
  Compute the diffusion model loss L_{DM} using Eq. 5
  Update π using the totatl loss L_{total} from Eq. 6
end for
return π

C Model Architecture

This section describes the model architectures used for all the experiments. Section C.1 presents the model architectures of BC, Implicit BC, Diffusion Policy, and our proposed framework DBC. Section C.2 details the model architectures of the EBM, VAE, and GAN used for the experiment comparing different generative models.

C.1 Model Architecture of BC, Implicit BC, Diffusion Policy, and DBC

We compare our DBC with three baselines (BC, Implicit BC, and Diffusion Policy) on various tasks in Section 5.3. We detail the model architectures for all the methods on all the tasks in Table 4. Note that all the models, the policy of BC, the energy-based model of Implicit BC, the conditional diffusion model of Diffusion Policy, the policy and the diffusion model of DBC, are parameterized by a multilayer perceptron (MLP). We report the implementation details for each method as follows.

Table 4: **Model Architectures.** We report the architectures used for all the methods on all the tasks.

Method	Models	Component	MAZE	FETCHPICK	FETCHPUSH	HANDROTATE	WALKER
BC	Policy π	# Layers	3	2	2	3	3
		Input Dim.	6	16	16	68	17
		Hidden Dim.	256	1024	1024	1024	256
		Output Dim.	2	4	3	20	6
Implicit BC	Policy π	# Layers	2	2	2	2	2
		Input Dim.	8	20	19	88	23
		Hidden Dim.	1024	1024	1024	512	1024
		Output Dim.	1	1	1	1	1
Diffusion Policy	Policy π	# Layers	5	5	5	5	5
		Input Dim.	8	20	19	88	23
		Hidden Dim.	256	1200	1024	2100	1200
		Output Dim.	2	4	3	20	6
DBC	DM ϕ	# Layers	5	5	5	5	5
		Input Dim.	8	20	19	88	23
		Hidden Dim.	128	1024	1024	2048	1024
		Output Dim.	8	20	19	88	23
	Policy π	# Layers	3	2	2	3	3
		Input Dim.	6	16	16	68	17
		Hidden Dim.	256	1024	1024	512	256
		Output Dim.	2	4	3	20	6

BC. The non-linear activation function is a hyperbolic tangent for all the BC policies. We experiment with BC policies with more parameters, which tend to severely overfit to expert datasets, resulting in worse performance.

Implicit BC. The non-linear activation function is ReLU for all energy-based models of Implicit BC. We empirically find that Implicit BC prefers shallow architectures in our tasks, so we set the number of layers to 2 for the energy-based models.

Diffusion Policy. The non-linear activation function is ReLU for all the policies of Diffusion Policy. We empirically find that Diffusion Policy performs better with a deeper architecture. Therefore, we set the number of layers to 5 for the policy. In most cases, we use a Diffusion Policy with more parameters than the total parameters of DBC consisting of the policy and the diffusion model.

DBC. The non-linear activation function is ReLU for the diffusion models and is a hyperbolic tangent for the policies. We apply batch normalization and dropout layers with a 0.2 ratio for the diffusion models on FETCHPICK and FETCHPUSH.

C.2 Model Architecture of EBM, VAE, and GAN

We compare different generative models (*i.e.*, EBM, VAE, and GAN) on MAZE in Section 5.5, and we report the model architectures used for the experiment in this section.

Energy-Based Model. An energy-based model (EBM) consists of 5 linear layers with ReLU activation. The EBM takes a concatenated state-action pair with a dimension of 8 as input; the output is a 1-dimensional vector representing the estimated energy values of the state-action pair. The size of the hidden dimensions is 128.

Variational Autoencoder. The architecture of a variational autoencoder consists of an encoder and a decoder. The inputs of the encoder are a concatenated state-action pair, and the outputs are the predicted mean and variance, which parameterize a Gaussian distribution. We apply the reparameterization trick [Kingma and Welling, 2014], sample features from the predicted Gaussian distribution, and use the decoder to produce the reconstructed state-action pair. The encoder and the decoder both consist of 5 linear layers with LeakyReLU Xu et al. [2020] activation. The size of the hidden dimensions is 128. That said, the encoder maps an 8-dimensional state-action pair to two 128-dimensional vectors (*i.e.*, mean and variance), and the decoder maps a sampled 128-dimensional vector back to an 8-dimensional reconstructed state-action pair.

Table 5: **Hyperparameters.** This table reports the hyperparameters used for all the methods on all the tasks. Note that our proposed framework (DBC) consists of two learning modules, the diffusion model and the policy, and therefore their hyperparameters are reported separately.

λ	Hyperparameter	MAZE	FETCHPICK	FETCHPUSH	HANDROTATE	WALKER
BC	Learning Rate	1e-4	1e-5	1e-5	5e-6	1e-4
	Batch Size	128	128	128	128	128
	# Epochs	2000	5000	5000	5000	2000
Implicit BC	Learning Rate	1e-4	5e-6	1e-4	1e-5	1e-4
	Batch Size	128	512	512	512	128
	# Epochs	10000	15000	15000	5000	10000
Diffusion Policy	Learning Rate	2e-4	1e-5	1e-5	1e-4	1e-4
	Batch Size	128	128	128	128	128
	# Epochs	20000	15000	15000	30000	10000
DBC (Ours)	Diffusion Model Learning rate	1e-3	1e-4	1e-4	3e-5	2e-4
	Diffusion Model Batch Size	128	128	128	128	1024
	Diffusion Model # Epochs	8000	10000	10000	10000	8000
	Policy Learning Rate	1e-4	1e-5	2e-5	1e-4	1e-4
	Policy Batch Size	128	128	128	128	128
	Policy # Epochs	2000	5000	5000	5000	2000
	λ	5	0.1	0.2	1	0.05

Generative Adversarial Network. The architecture of the generative adversarial network consists of a generator and a discriminator. The generator is the policy model that predicts an action from a given state, whose input dimension is 6 and output dimension is 2. On the other hand, the discriminator learns to distinguish the expert state-action pairs (s, a) from the state-action pairs produced by the generator $(s, \hat{a})$. Therefore, the input dimension of the discriminator is 8, and the output is a scalar representing the probability of the state-action pair being "real." The generator and the discriminator both consist of three linear layers with ReLU activation, and the size of the hidden dimensions is 256.

D Training and Inference Details

We describe the details of training and performing inference in this section, including computation resources and hyperparameters.

D.1 Computation Resource

We conducted all the experiments on the following three workstations:

- M1: ASUS WS880T workstation with an Intel Xeon W-2255 (10C/20T, 19.25M, 4.5GHz) 48-Lane CPU, 64GB memory, an NVIDIA RTX 3080 Ti GPU, and an NVIDIA RTX 3090 Ti GPU
- M2: ASUS WS880T workstation with an Intel Xeon W-2255 (10C/20T, 19.25M, 4.5GHz) 48-Lane CPU, 64GB memory, an NVIDIA RTX 3080 Ti GPU, and an NVIDIA RTX 3090 Ti GPU
- M3: ASUS WS880T workstation with an Intel Xeon W-2255 (10C/20T, 19.25M, 4.5GHz) 48-Lane CPU, 64GB memory, and two NVIDIA RTX 3080 Ti GPUs

D.2 Hyperparamters

We report the hyperparameters used for all the methods on all the tasks in Table 5. We use the Adam optimizer Kingma and Ba [2015] for all the methods on all the tasks and use linear learning rate decay for all policy models.

D.3 Inference Details

This section describes how each method infers an action $\hat{a}$ given a state s.

BC & DBC. The policy models of BC and DBC can directly predict an action given a state, *i.e.*, $\hat{a} \sim \pi(s)$, and are therefore more efficient during inference as described in Section 5.3.

Implicit BC. The energy-based model (EBM) of Implicit BC learns to predict an estimated energy value for a state-action pair during training. To generate a predicted $\hat{a}$ given a state s during inference, it requires a procedure to sample and optimize actions. We follow Florence et al. [2022] and implement a derivative-free optimization algorithm to perform inference.

The algorithm first randomly samples N_s vectors from the action space as candidates. The EBM then produces the estimated energy value of each candidate action and applies the Softmax function on the estimated energy values to produce a N_s-dimensional probability. Then, it samples candidate actions according to the above probability and adds noise to them to generate another N_s candidates for the next iteration. The above procedure iterates N_{iter} times. Finally, the action with maximum probability in the last iteration is selected as the predicted action $\hat{a}$. In our experiments, N_s is set to 1000 and N_{iter} is set to 3.

Diffusion Policy. Diffusion Policy learns a conditional diffusion model as a policy and produces an action from sampled noise vectors conditioning on the given state during inference. We follow Pearce et al. [2023], Chi et al. [2023] and adopt Denoising Diffusion Probabilistic Models (DDPMs) J Ho [2020] for the diffusion models. Once learned, the diffusion policy π can "denoise" a noise sampled from a Gaussian distribution $\mathcal{N}(0, 1)$ given a state s and yield a predicted action $\hat{a}$ using the following equation:

$$a_{n-1} = \frac{1}{\sqrt{\alpha_n}}(a_n - \frac{1-\alpha_n}{\sqrt{1-\bar{\alpha}_n}}\pi(s, a_n, n)) + \sigma_n z, \tag{7}$$

where α_n, $\bar{\alpha}_n$, and σ_n are schedule parameters, n is the current time step of the reverse diffusion process, and $z \sim \mathcal{N}(0, 1)$ is a random vector. The above denoising process iterates N times to produce a predicted action a_0 from a sampled noise $a_N \sim \mathcal{N}(0, 1)$. The number of total diffusion steps N is 100 in our experiment, which is the same for the diffusion model in DBC.

D.4 Comparing Different Generative Models

Our proposed framework employs a diffusion model (DM) to model the joint probability of expert state-action pairs and utilizes it to guide policy learning. To justify our choice of generative models, we explore using other popular generative models to replace the diffusion model in MAZE. Specifically, we consider energy-based models (EBMs) [Du and Mordatch, 2019, Song and Kingma, 2021], variational autoencoders (VAEs) [Kingma and Welling, 2014], and generative adversarial networks (GANs) Goodfellow et al. [2014]. Each generative model learns to model the joint distribution of expert state-action pairs. For fair comparisons, all the policy models learning from learned generative models consists of 3 linear layers with ReLU activation, where the hidden dimension is 256. All the policies are trained for 2000 epochs using the Adam optimizer [Kingma and Ba, 2015], and a linear learning rate decay is applied for EBMs and VAEs.

D.4.1 Energy-Based Model

Model Learning. Energy-based models (EBMs) learn to model the joint distribution of the expert state-action pairs by predicting an estimated energy value for a state-action pair (s, a). The EBM aims to assign low energy value to the real expert state-action pairs while high energy otherwise. Therefore, the predicted energy value can be used to evaluate how well a state-action pair (s, a) fits the distribution of the expert state-action pair distribution.

To train the EBM, we generate N_{neg} random actions as negative samples for each expert state-action pair as proposed in Florence et al. [2022]. The objective of the EBM E_ϕ is the InfoNCE loss Oord et al. [2018]:

$$\mathcal{L}_{\text{InfoNCE}} = \frac{e^{-E_\phi(s,a)}}{e^{-E_\phi(s,a)} + \Sigma_{i=1}^{N_{neg}} e^{-E_\phi(s,\tilde{a}_i)}}, \tag{8}$$

where (s, a) indicates an expert state-action pair, $\tilde{a}_i$ indicates the sampled random action, and N_{neg} is set to 64 in our experiments. The EBM learns to separate the expert state-action pairs from the negative samples by optimizing the above InfoNCE loss.

The EBM is trained for 8000 epochs with the Adam optimizer [Kingma and Ba, 2015], with a batch size of 128 and an initial learning rate of 0.0005. We apply learning rate decay by 0.99 for every 100 epoch.

Guiding Policy Learning. To guide a policy π to learn, we design an EBM loss $\mathcal{L}_{\text{EBM}} = E_\phi(s, \hat{a})$, where $\hat{a}$ indicates the predicted action produced by the policy. The above EBM loss regularizes the policy to generate actions with low energy values, which encourage the predicted state-action pair $(s, \hat{a})$ to fit the modeled expert state-action pair distribution. The policy learning from this EBM loss $\mathcal{L}_{\text{EBM}}$ achieves a success rate of 49.09% in MAZE as reported in Table 2.

We also experiment with combining this EBM loss $\mathcal{L}_{\text{EBM}}$ with the $\mathcal{L}_{\text{BC}}$ loss. The policy optimizes $\mathcal{L}_{\text{BC}} + \lambda_{\text{EBM}}\mathcal{L}_{\text{EMB}}$, where λ_{EBM} is set to 0.1. Optimizing this combined loss yields a success rate of 80.00% in MAZE as reported in Table 2.

D.4.2 Variational Autoencoder

Model Learning. Variational autoencoders (VAEs) model the joint distribution of the expert data by learning to reconstruct expert state-action pairs (s, a). Once the VAE is learned, how well a state-action pair fits the expert distribution can be reflected in the reconstruction loss.

The objective of training a VAE is as follows:

$$\mathcal{L}_{\text{vae}} = ||\hat{x} - x||^2 + D_{\text{KL}}(\mathcal{N}(\mu_x, \sigma_x)||\mathcal{N}(0, 1)), \tag{9}$$

where x is the latent variable, *i.e.*, the concatenated state-action pair $x = [s, a]$, and $\hat{x}$ is the reconstruction of x, *i.e.*, the reconstructed state-action pair. The first term is the reconstruction loss, while the second term encourages aligning the data distribution with a normal distribution $\mathcal{N}(0, 1)$, where μ_x and σ_x are the predicted mean and standard deviation given x.

The VAE is trained for $100k$ update iterations with the Adam optimizer [Kingma and Ba, 2015], with a batch size of 128 and an initial learning rate of 0.0001. We apply learning rate decay by 0.5 for every $5k$ epoch.

Guiding Policy Learning. To guide a policy π to learn, we design a VAE loss $\mathcal{L}_{\text{VAE}} = max(\mathcal{L}_{\text{vae}}^{\text{agent}} - \mathcal{L}_{\text{vae}}^{\text{expert}}, 0)$, similar to Eq. 5. This loss forces the policy to predict an action, together with the state, that can be well reconstructed with the learned VAE. The policy learning from this VAE loss $\mathcal{L}_{\text{VAE}}$ achieves a success rate of 48.47% in MAZE as reported in Table 2.

We also experiment with combining this VAE loss $\mathcal{L}_{\text{VAE}}$ with the $\mathcal{L}_{\text{BC}}$ loss. The policy optimizes $\mathcal{L}_{\text{BC}} + \lambda_{\text{VAE}}\mathcal{L}_{\text{VAE}}$, where λ_{VAE} is set to 1. Optimizing this combined loss yields a success rate of 82.31% in MAZE as reported in Table 2.

D.4.3 Generative Adversarial Network

Adversarial Model Learning & Policy Learning. Generative adversarial networks (GANs) model the joint distribution of expert data with a generator and a discriminator. The generator aims to synthesize a predicted action $\hat{a}$ given a state s. On the other hand, the discriminator aims to identify expert the state-action pair (s, a) from the predicted one $(s, \hat{a})$. Therefore, a learned discriminator can evaluate how well a state-action pair fits the expert distribution.

While it is possible to learn a GAN separately and utilize the discriminator to guide policy learning, we let the policy π be the generator directly and optimize the policy with the discriminator iteratively. We hypothesize that a learned discriminator may be too selective for a policy training from scratch, so we learn the policy π with the discriminator D to improve the policy and the discriminator simultaneously.

The objective of training the discriminator D is as follows:

$$\mathcal{L}_{\text{disc}} = BCE(D(s, a), 1) + BCE(D(s, \hat{a}), 0) = -log(D(s, a)) - log(1 - D(s, \hat{a})), \tag{10}$$

where $\hat{a} = \pi(s)$ is the predicted action, and BCE is the binary cross entropy loss. The binary label $(0, 1)$ indicates whether or not the state-action pair sampled from the expert data. The generator and the discriminator are both updated by Adam optimizers using a 0.00005 learning rate.

To learn a policy (*i.e.*, generator), we design the following GAN loss:

$$\mathcal{L}_{\text{GAN}} = BCE(D(s, \hat{a}), 1) = -log(D(s, \hat{a})). \tag{11}$$

Table 6: **FETCHPICK Generalization Experimental Result.** We report the performance of our proposed framework DBC and the baselines regarding the mean and the standard deviation of the success rate with different levels of noise injected into the initial state and goal locations in FETCHPICK, evaluated over three random seeds.

Method	Noise Level				
	1	1.25	1.5	1.75	2
BC	86.78% ± 4.68%	69.15% ± 5.00%	54.42% ± 3.89%	43.49% ± 4.68%	36.64% ± 3.85%
Implicit BC	89.40% ± 4.85%	72.27% ± 6.71%	46.32% ± 5.49%	34.60% ± 4.78%	25.84% ± 4.16%
Diffusion Policy	76.04% ± 3.12%	74.37% ± 3.80%	69.22% ± 5.23%	56.95% ± 4.63%	53.93% ± 4.49%
DBC (Ours)	**97.59%** ± 1.53%	**88.71%** ± 6.46%	**78.76%** ± 10.84%	**69.36%** ± 12.72%	**62.62%** ± 14.01%

Table 7: **FETCHPUSH Generalization Experimental Result.** We report the performance of our proposed framework DBC and the baselines regarding the mean and the standard deviation of the success rate with different levels of noise injected into the initial state and goal locations in FETCHPUSH, evaluated over three random seeds.

Method	Noise Level				
	1	1.25	1.5	1.75	2
BC	94.07% ± 4.45%	82.52% ± 5.46%	66.02% ± 6.88%	48.85% ± 8.65%	34.82% ± 7.13%
Implicit BC	85.95% ± 8.39%	83.99% ± 6.06%	77.70% ± 4.42%	70.33% ± 6.06%	56.98% ± 11.74%
Diffusion Policy	97.92% ± 1.10%	93.02% ± 2.36%	86.93% ± 3.26%	74.50% ± 3.66%	65.84% ± 3.81%
DBC (Ours)	**99.83%** ± 0.23%	**99.38%** ± 0.78%	**94.92%** ± 3.09%	**87.48%** ± 5.04%	**78.43%** ± 7.41%

The above GAN loss guides the policy to generate state-action pairs that fit the joint distribution of the expert data. The policy learning from this GAN loss $\mathcal{L}_{\text{GAN}}$ achieves a success rate of 50.29% in MAZE as reported in Table 2.

We also experiment with combining this GAN loss $\mathcal{L}_{\text{GAN}}$ with the $\mathcal{L}_{\text{BC}}$ loss. The policy optimizes $\mathcal{L}_{\text{BC}} + \lambda_{\text{GAN}}\mathcal{L}_{\text{GAN}}$, where λ_{GAN} is set to 0.2. Optimizing this combined loss yields a success rate of 71.64% in MAZE as reported in Table 2.

E Generalization Experiments in FETCHPICK and FETCHPUSH

This section further investigates the generalization capabilities of the policies learned by our proposed framework and the baselines. To this end, we evaluate the policies by injecting different noise levels to both the initial state and goal location in FETCHPICK and FETCHPUSH. Specifically, we parameterize the noise by scaling the 2D sampling regions for the block and goal locations in both environments. We expect all the methods to perform worse with higher noise levels, while the performance drop of the methods with better generalization ability is less significant. The results are presented in Table 6 for FETCHPICK and Table 7 for FETCHPUSH.

Overall Performance. Our proposed framework DBC consistently outperforms all the baselines with different noise levels, indicating the superiority of DBC when different levels of generalization are required.

Performance Drop with Increased Noise Level. In FETCHPICK, DBC experiences a performance drop of 35.0% when the noise level increase from 1 to 2. However, BC and Implicit BC demonstrate a more significant performance drop of 50.1% and 63.6%, respectively. Notably, Diffusion Policy initially performs poorly at a noise level of 1 but demonstrates its robustness with a performance drop of only 22.1% when the noise level increases to 2. On the other hand, in FETCHPUSH, DBC experiences a performance drop of 21.4% when the noise level increase from 1 to 2, while all the baselines have a more significant performance drop: BC (63%), Implicit BC (33.7%), and Diffusion Policy (32.8%). This demonstrates that our proposed framework not only generalizes better but also exhibits greater robustness to noise compared to the baselines.

In this experiment, we set the coefficient λ of DBC to 0.5 in FETCHPUSH and 0.1 in FETCHPICK, resulting in improved performance compared to the performance reported in the main paper.

In this experiment, we set the coefficient λ of DBC to 0.5 in FETCHPUSH and 0.1 in FETCHPICK, resulting in an improved performance compared to the performance reported in the main paper.

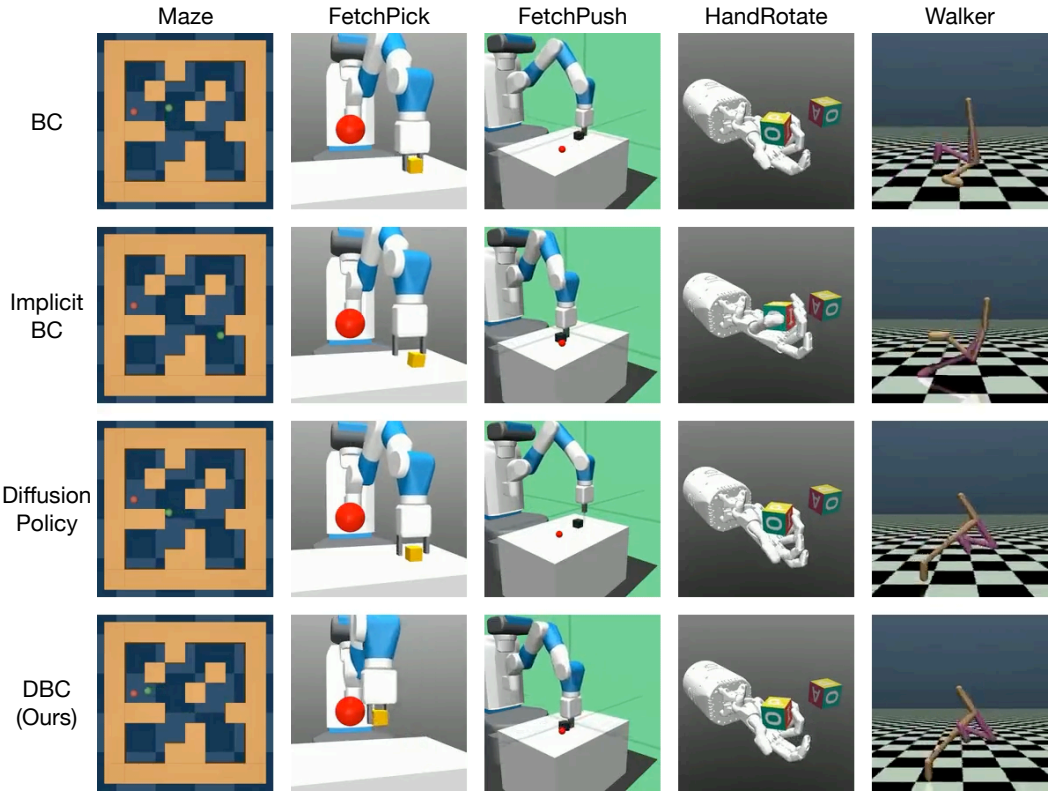

Figure 5: **Qualitative Results.** Rendered videos of the policies learned by our proposed framework and the baselines can be found at https://sites.google.com/view/diffusion-behavioral-cloning.

F Qualitative Results and Additional Analysis

This section provides more detailed analyses of our proposed framework and the baselines. We present the qualitative results in Section F.1. Then, we analyze the learning progress and the episode length of goal-directed tasks during inference in Section F.2 and Section F.3, respectively.

F.1 Qualitative Results

Rendered videos of the policies learned by our proposed framework and the baselines can be found at https://sites.google.com/view/diffusion-behavioral-cloning. A screenshot of the rendered videos on the web page is presented in Figure 5.

F.2 Learning Progress Analysis

In this section, we analyze the learning progress of all the methods on all the tasks. The training curves are presented in Figure 6. Our proposed framework (DBC) not only achieves the best converged performance but also converges the fastest, demonstrating its learning efficiency.

Since Implicit BC and Diffusion Policy take significantly longer to converge, we set a higher number of training epochs for these two methods (see Table 5), and hence their learning curves are notably longer than BC and DBC.

Note that we make sure the numbers of training epochs for Implicit BC and Diffusion Policy are not less the total number of training epochs for learning both the diffusion model and the policy in DBC, except for Implicit BC in HANDROTATE where training longer does not yield any improvement. This forecloses the possibility of the superior performance of DBC coming from learning with a higher total number of training epochs.

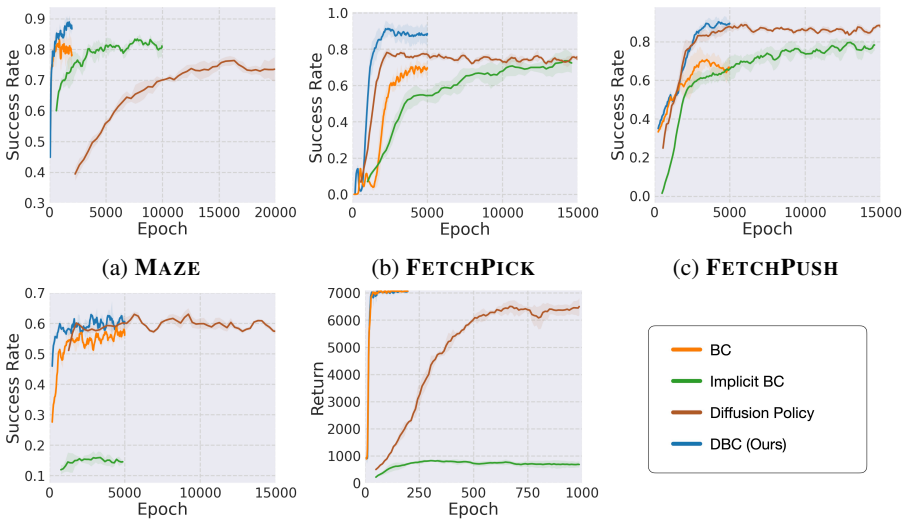

(a) MAZE (b) FETCHPICK (c) FETCHPUSH

(d) HANDROTATE (e) WALKER

Figure 6: **Learning Progress.** We evaluate the baselines and our proposed method DBC and its variants during the learning process. Since Implicit BC (green) and Diffusion Policy (brown) take significantly longer to converge, we set a higher number of training epochs for these two methods, and hence their learning curves are notably longer than BC (orange) and DBC (blue). Our method demonstrates superior learning efficiency over the baselines.

F.3 Episode Length Analysis of Goal-Directed Tasks

In this section, we investigate the efficiency of the learned policies regarding the number of time steps they need to fulfill a task. We compare all the methods regarding average episode lengths over 100 episodes and three random seeds in all goal-directed tasks (MAZE, FETCHPUSH, FETCHPICK, and HANDROTATE). The results are presented in Table 8 and Figure 7.

Note that Implicit BC and Diffusion Policy take significantly longer to converge, and hence we set a higher number of training epochs for these two methods (see Table 5). As a result, their learning curves are notably longer than BC and DBC.

We observe that our proposed framework DBC results in the shortest episode lengths in MAZE, FETCHPUSH, and FETCHPICK while performing competitively against the best-performing baseline (Diffusion Policy) in HANDROTATE. This indicates that DBC learns an efficient policy that can accomplish tasks quickly.

G On the Theoretical Motivation for Guiding Policy Learning with Diffusion Model

This section further elaborates on the technical motivation for leveraging diffusion models for imitation learning. Specifically, we aim to learn a diffusion model to model the joint distribution of expert state-action pairs. Then, we propose to utilize this learned diffusion model to augment a BC policy that aims to imitate expert behaviors.

We consider the distribution of expert state-action pairs as the real data distribution q_x in learning a diffusion model. Following this setup, x_0 represents an original expert state-action pair (s, a) and $q(x_n|x_{n-1})$ represents the forward diffusion process, which gradually adds Gaussian noise to the data in each timestep $n = 1, ..., N$ until x_N becomes an isotropic gaussian distribution. On the other hand, the reverse diffusion process is defined as $\phi(x_{n-1}|x_n) := \mathcal{N}(x_{n-1}; \mu_\theta(x_n, n), \Sigma_\theta(x_n, n))$, where θ denotes the learnable parameters of the diffusion model ϕ, as illustrated in Figure 1.

Our key idea is to use the proposed diffusion model loss $\mathcal{L}_{\text{DM}}$ in Eq. 5 as an estimate of how well a predicted state-action pair $(s, \hat{a})$ fits the expert state-action pair distribution, as described in Section 4.2.2. In the following derivation, we will show that by optimizing this diffusion model loss $\mathcal{L}_{\text{DM}}$, we

Table 8: **Episode Length of Goal-Directed Tasks.** We report the mean and the standard deviation of the episode length (↓) on MAZE, FETCHPICK, FETCHPUSH, and HANDROTATE, evaluated over three random seeds. The experiments demonstrate that our proposed method (DBC) outperforms (*i.e.*, finish tasks with fewer time steps) the baselines on MAZE, FETCHPICK, and FETCHPUSH while performing competitively in HANDROTATE.

Method	MAZE	FETCHPICK	FETCHPUSH	HANDROTATE
BC	219.95 ± 13.21	39.92 ± 0.65	74.08 ± 5.55	33.79 ± 1.18
Implicit BC	199.91 ± 15.95	44.67 ± 0.65	67.75 ± 3.13	46.13 ± 0.84
Diffusion Policy	241.45 ± 12.47	42.20 ± 0.64	80.93 ± 8.88	**31.95** ± 0.82
DBC (Ours)	**193.12** ± 10.30	**30.22** ± 1.38	**54.58** ± 3.33	**31.97** ± 1.49

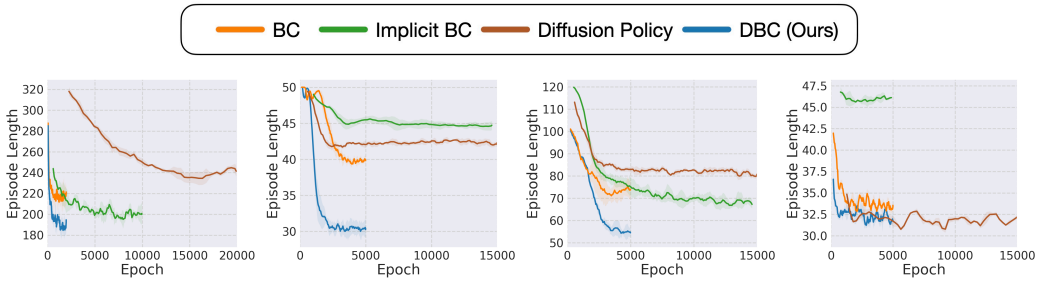

(a) **MAZE** (b) **FETCHPICK** (c) **FETCHPUSH** (d) **HANDROTATE**

Figure 7: **Episode Length of Goal-Directed Tasks.** We evaluate the baselines and our proposed method regarding the episode length during the learning process. Since Implicit BC (green) and Diffusion Policy (brown) take significantly longer to converge, we set a higher number of training epochs for these two methods, and hence their learning curves are notably longer than BC (orange) and DBC (blue). The average episode length indicates how fast the agent reaches the goal, which can be a measurement of the efficiency of the agent. Our method DBC demonstrates superior efficiency in accomplishing tasks.

maximize the lower bound of the agent data's probability under the derived expert distribution and hence bring the agent policy π closer to the expert policy π^E, which is the goal of imitation learning.

As depicted in [Luo [2022]], one can conceptualize diffusion models, including DDPM [J Ho, 2020] adopted in this work, as a hierarchical variational autoencoder [Kingma and Welling, 2014], which maximizes the likelihood $p(x)$ of observed data points x. Therefore, similar to hierarchical variational autoencoders, diffusion models can optimize the Evidence Lower Bound (ELBO) by minimizing the KL divergence $D_{KL}(q(x_{n-1}|x_n, x_0)||\phi(x_{n-1}|x_n))$. Consequently, this can be viewed as minimizing the KL divergence to fit the distribution of the predicted state-action pairs $(s, \hat{a})$ to the distribution of expert state-action pairs.

According to Bayes' theorem and the properties of Markov chains, the forward diffusion process $q(x_{n-1}|x_n, x_0)$ follows:

$$q(x_{n-1}|x_n, x_0) \sim \mathcal{N}(x_{n-1}; \underbrace{\frac{\sqrt{\alpha_n}(1-\bar{\alpha}_{n-1})x_n + \sqrt{\bar{\alpha}_{n-1}}(1-\alpha_n)x_0}{1-\bar{\alpha}_n}}_{\mu_q(x_n, x_0),} \underbrace{\frac{(1-\alpha_n)(1-\bar{\alpha}_{n-1})}{1-\bar{\alpha}_n}}_{\Sigma_q(n)}).$$

The variation term $\Sigma_q(n)$ in the above equation can be written as $\sigma_q^2(n)I$, where $\sigma_q^2(n) = \frac{(1-\alpha_n)(1-\bar{\alpha}_{n-1})}{1-\bar{\alpha}_n}$. Therefore, minimizing the KL divergence is equivalent to minimizing the gap

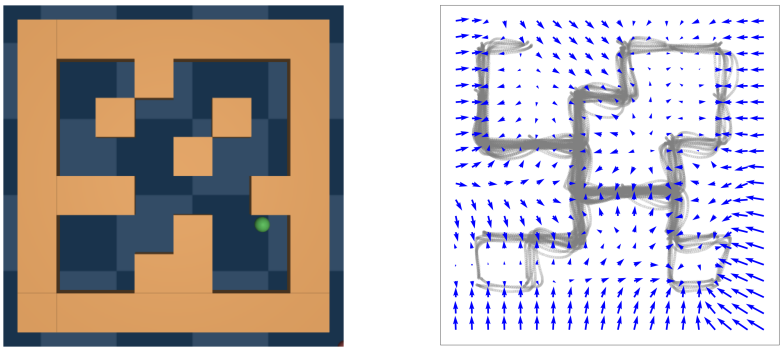

(a) **Maze Layout** (b) **Learned Gradient Field**

Figure 8: **Visualized Gradient Field. (a) Maze Layout**: The layout of the medium maze used for MAZE. **(b) Learned Gradient Field**: We visualize the MAZE expert demonstration as a distribution of points by their first two dimensions in gray. The points that cluster densely have a high probability, and vice versa. Once a diffusion model is well-trained, it can move randomly sampled points to the area with high probability by predicting gradients (blue arrows). Accordingly, the estimate $p(s, a)$ of joint distribution modeling can serve as guidance for policy learning, as proposed in this work.

between the mean values of the two distributions:

$$\begin{aligned}
&\arg\min_{\theta} D_{KL}(q(x_{n-1}|x_n, x_0)||\phi(x_{n-1}|x_n)) \\
&= \arg\min_{\theta} D_{KL}(\mathcal{N}(x_{n-1}; \mu_q, \Sigma_q(n))||\mathcal{N}(x_{n-1}; \mu_\theta, \Sigma_q(n))) \\
&= \arg\min_{\theta} \frac{1}{2\sigma_q^2(n)}[||\mu_\theta - \mu_q||_2^2],
\end{aligned}$$

where μ_q represents the denoising transition mean and μ_θ represents the approximated denoising transition mean by the model.

Different implementations adopt different forms to model μ_θ. Specifically, for DDPMs adopted in this work, the true denoising transition mean $\mu_q(x_n, x_0)$ derived above can be rewritten as:

$$\mu_q(x_n, x_0) = \frac{1}{\sqrt{\alpha_n}}(x_n - \frac{1-\alpha_n}{\sqrt{1-\bar{\alpha}_n}}\epsilon_0),$$

which is referenced from Eq. 11 in J Ho [2020]. Hence, we can set our approximate denoising transition mean μ_θ in the same form as the true denoising transition mean:

$$\mu_\theta(x_n, n) = \frac{1}{\sqrt{\alpha_n}}(x_n - \frac{1-\alpha_n}{\sqrt{1-\bar{\alpha}_n}}\hat{\epsilon_\theta}(x_n, n)), \tag{12}$$

as illustrated in Popov et al. [2022]. Song et al. [2021] further show that the entire diffusion model formulation can be revised to view continuous stochastic differential equations (SDEs) as a forward diffusion. It points out that the reverse process is also an SDE, which can be computed by estimating a score function $\nabla_x \log p_t(x)$ at each denoising time step. The idea of representing a distribution by modeling its score function is introduced in Song and Ermon [2019]. The fundamental concept is to model the gradient of the log probability density function $\nabla_x \log p_t(x)$, a quantity commonly referred to as the (Stein) score function. Such score-based models are not required to have a tractable normalizing constant and can be directly acquired through score matching. The measure of this score function determines the optimal path to take in the space of the data distribution to maximize the log probability under the derived real distribution.

As shown in Figure 8b, we visualized the learned gradient field of a diffusion model, which learns to model the expert state-action pairs in MAZE. Once trained, this diffusion model can guide a policy with predicted gradients (blue arrows) to move to areas with high probability, as proposed in our work.

Essentially, by moving in the opposite direction of the source noise, which is added to a data point x_t to corrupt it, the data point is "denoised"; hence the log probability is maximized. This is supported

by the fact that modeling the score function is the same as modeling the negative of the source noise. This perspective of the diffusion model is dubbed diffusion SDE. Moreover, Popov et al. [2022] prove that Eq. 12 is diffusion SDE's maximum likelihood SDE solver. Hence, the corresponding divergence optimization problem can be rewritten as:

$$\begin{aligned}&\arg\min_{\theta} D_{KL}(q(x_{n-1}|x_n, x_0)||\phi(x_{n-1}|x_n))\\&= \arg\min_{\theta} \frac{1}{2\sigma_q^2(n)} \frac{(1-\alpha_n)^2}{(1-\bar{\alpha}_n)\alpha_n}[||\hat{\epsilon}_\theta(x_n, n) - \epsilon_0||_2^2],\end{aligned}$$

where ϵ_θ is a function approximator aim to predict ϵ from x. As the coefficients can be omitted during optimization, we yield the learning objective $\mathcal{L}_{\text{diff}}$ as stated in in Eq. 2:

$$\mathcal{L}_{\text{diff}} = ||\hat{\epsilon}(s, a, n) - \epsilon(n)||^2 = ||\phi(s, a, \epsilon(n)) - \epsilon(n)||^2.$$

The above derivation motivates our proposed framework that augments a BC policy by using the diffusion model to provide guidance that captures the joint probability of expert state-action pairs. Based on the above derivation, minimizing the proposed diffusion model loss (*i.e.*, learning to denoise) is equivalent to finding the optimal path to take in the data space to maximize the log probability. To be more accurate, when the learner policy predicts an action that obtains a lower $\mathcal{L}_{\text{diff}}$, it means that the predicted action $\hat{a}$, together with the given state s, fits better with the expert distribution.

Accordingly, by minimizing our proposed diffusion loss, the policy is encouraged to imitate the expert policy. To further alleviate the impact of rarely-seen state-action pairs (s, a), we propose to compute the above diffusion loss for both expert data (s, a) and predicted data $(s, \hat{a})$ and yield $\mathcal{L}_{\text{diff}}^{\text{expert}}$ and $\mathcal{L}_{\text{diff}}^{\text{agent}}$, respectively. Therefore, we propose to augment BC with this objective: $\mathcal{L}_{\text{DM}} = max(\mathcal{L}_{\text{diff}}^{\text{agent}} - \mathcal{L}_{\text{diff}}^{\text{expert}}, 0)$ This design is justified in Section 5.6.2.

H Limitations

This section discusses the limitations of our proposed framework.

- Since this work aims to learn from demonstrations without interacting with environments, our proposed framework in its current form is only designed to learn from expert trajectories and cannot learn from trajectories produced by the learner policy. Extending our method to incorporate agent data can potentially allow for improvement when interacting environments are possible, which is left for future work.
- The key insight of our work is to allow the learner policy to benefit from both modeling the conditional and joint probability of expert state-action distributions. To this end, we propose to optimize both the BC loss and the proposed diffusion model loss. To balance the importance of the two losses, we introduce a coefficient λ as an additional hyperparameter. While the ablation study conducted in MAZE shows that the performance of our proposed framework is robust to λ, this can potentially increase the difficulty of searching for optimal hyperparameters when applying our proposed framework to a new application.

I Broader Impacts

This work proposes Diffusion Model-Augmented Behavioral Cloning, a novel imitation learning framework that aims to increase the ability of autonomous learning agents (*e.g.*, robots, game AI agents) to acquire skills by imitating demonstrations provided by experts (*e.g.*, humans). However, it is crucial to acknowledge that our proposed framework, by design, inherits any biases exhibited by the expert demonstrators. These biases can manifest as sub-optimal, unsafe, or even discriminatory behaviors. To address this concern, ongoing research endeavors to mitigate bias and promote fairness in machine learning hold promise in alleviating these issues. Moreover, research works that enhance learning agents' ability to imitate experts, such as this work, can pose a threat to job security. Nevertheless, in sum, we firmly believe that our proposed framework can offer tremendous advantages in terms of enhancing the quality of human life and automating laborious, arduous, or perilous tasks that pose risks to humans, which far outweigh the challenges and potential issues.